

# Hydride formation on the platelet inner surface of plasma-hydrogenated crystalline silicon investigated with Raman spectroscopy

Y. Ma, Y. L. Huang, W. Dungen, R. Job, and W. R. Fahrner

Chair of Electronic Devices, University of Hagen, Haldener Strasse 182, P.O. Box 940, D-58084 Hagen, Germany

(Received 21 March 2005; published 8 August 2005)

Phosphorous-doped Czochralski silicon wafers are hydrogenated with a plasma enhanced chemical vapor deposition setup. Platelets are created during the H-plasma treatments. The hydride formation on the inner surfaces of the platelets is investigated with depth-resolved micro-Raman spectroscopy. Several Si-H Raman subpeaks at 2065, 2075, 2120, 2130, and 2140  $\text{cm}^{-1}$  are found to be related to the different growth stages of the platelets. The formation of the platelet starts with the  $[2\text{Si-H}]_n$  structure without  $\text{H}_2$  molecules inside. During the platelet growth  $\text{H}_2$  molecules are formed inside and the inner surfaces of the platelets become flatter and less defective.

DOI: [10.1103/PhysRevB.72.085321](https://doi.org/10.1103/PhysRevB.72.085321)

PACS number(s): 68.35.Dv, 78.30.Am, 81.15.Gh, 33.20.Fb

## I. INTRODUCTION

The observation of the platelet formation in hydrogenated crystalline silicon (*c*-Si) can be traced back to the late 1980s, when Johnson *et al.* found that the H-plasma treatment of *c*-Si materials induced platelets, which were not related to the plasma or radiation damage.<sup>1</sup> A number of investigations were then carried out to study the microscopic structure of the platelets and the impact of some parameters such as substrate temperature,<sup>2-5</sup> post-hydrogenation annealing,<sup>6-9</sup> disorder,<sup>10-12</sup> doping type, and Fermi-level position<sup>1,13-15</sup> on the formation of the platelets in Si. However, most of these investigations were done with remote H-plasma treatments, which were more relevant to the plasma cleaning process from an application point of view. On the other hand, hydrogen is also an important (even dominant in some cases) gas in some plasma sources commercially used in semiconductor industries, such as reactive ion etching and plasma enhanced chemical vapor deposition (PECVD). Little investigation has been done on the platelet formation in *c*-Si material during these treatments. In this study the hydrogenation was done with a PECVD setup under conditions similar as for *a*-Si:H or *mc*-Si:H deposition (with respect to substrate temperature, plasma power, hydrogen gas flux, and chamber pressure, etc.).

Raman spectroscopy (RS) investigations show that the inner surfaces of platelets are passivated by Si-H bonds; and  $\text{H}_2$  molecules are formed in the open space of the platelets.<sup>5,9,13,16-18</sup> Si-H bonds formed on *c*-Si surfaces have been extensively studied since the past decades with optical<sup>19-30</sup> and nuclear methods.<sup>31,32</sup> Some of Si-H species have been distinguished according to their specific vibration frequency. For these investigations infrared (IR) spectroscopy is the main tool. It is found that not only different indices,  $n$ , in  $\text{SiH}_n$ , but also different configurations of the neighboring Si-H bonds, will result in different Si-H vibration frequencies.<sup>24,26,30</sup> On the other hand, RS is more efficient to detect  $\text{H}_2$  molecules, which can be considered as the fingerprint for platelets. Therefore the combination of Si-H bond and  $\text{H}_2$  molecule Raman spectra can identify those Si-H species located at the inner surfaces of the platelets. Ac-

ording to the local vibration modes of the Si-H bonds, the microscopic structure of the platelets can be subsequently deduced. In our previous investigations we have studied two Raman subpeaks at 2105 and 2110  $\text{cm}^{-1}$ , which were assigned to the dihydride ( $\text{SiH}_2$ ) at the inner surfaces of the platelets.<sup>8,9,18</sup> In this study we extend the above investigations to other Si-H subpeaks at 2065, 2075, 2120, 2130, and 2140  $\text{cm}^{-1}$ , which all are located inside the platelets but stem from different hydride species.

## II. EXPERIMENT

The investigations were carried out on phosphorous-doped [100]-oriented Czochralski Si wafers with a thickness of  $\sim 400 \mu\text{m}$ , a diameter of 3 in. and a resistivity of 9–11  $\Omega \text{ cm}$ . H-plasma treatments were done in a PECVD setup at a frequency of 13.56 MHz, a power of 10 W, a substrate temperature of 260  $^\circ\text{C}$ , a hydrogen flux of 200 sccm, a pressure of 2000 mTorr, and for various durations. The samples treated for 5, 10, 20, and 60 min were labeled with S1, S2, S3, and S4, respectively. The wafer was directly attached facedown on the top electrode. The wafer and both electrodes were horizontally mounted inside the chamber. The distance between two electrodes was about 1.5 cm. The maximum dimension of the sample was  $10 \times 10 \text{ cm}^2$ . After H-plasma treatment, the samples were cut into  $1 \times 1 \text{ cm}^2$  pieces, then annealed on a hot stage and/or mechanically beveled with a small angle (about  $0.5^\circ$ ). We found that no Si-H bonds or  $\text{H}_2$  molecules were formed during the beveling process.

Micro-RS was carried out on the beveled surfaces of the samples so that the Raman spectra of different sample depths could be obtained. The method of depth-resolved  $\mu\text{RS}$  has been successfully demonstrated elsewhere.<sup>18</sup> Its main advantage was that the depth profiles of various Si-H or  $\text{H}_2$  species could be distinguished easily due to their different Raman shifts. The excitation of the RS was supplied by an  $\text{Ar}^+$  ion laser (488 nm, 40 mW). The spectra were collected at room temperature by a Peltier cooled CCD detector. The spectral range was from 200 to 4600  $\text{cm}^{-1}$ , with a resolution limited to  $\sim 1 \text{ cm}^{-1}$ . The spectra were normalized with the

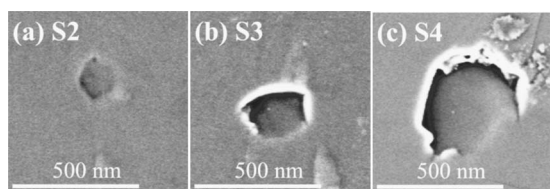


FIG. 1. SEM images of platelets observed on the beveled surface of the samples hydrogenated for (a) 10 min, S2, (b) 20 min, S3, and (c) 60 min, S4. The magnification is 50 000.

*c*-Si optical phonon line ( $\sim 520 \text{ cm}^{-1}$ ). A LEO 982 scanning electron microscope (SEM) was employed on the beveled surfaces of the samples to observe the platelets. The applied voltage was 1 keV, and the work distance was about 3 mm.

### III. RESULTS

Shown in Figs. 1(a)–1(c) are the SEM images of the platelets lying at a depth of about  $0.3 \mu\text{m}$  in S2 (10 min H-plasma treatment), S3 (20 min), and S4 (60 min), respectively. Although RS measurements show that platelets are already formed in S1 (5 min), no platelets are detectable with the SEM, i.e., the diameter of the platelets in this sample should be similar to or less than the order of  $\sim 10 \text{ nm}$  (determined by the SEM resolution). As shown in Fig. 1, it is evident that the diameter of the platelets increases with the H-plasma duration, i.e., in the average from about 150 to 400 nm when the H-plasma duration increases from 10 to 60 min. With higher H-plasma power (50 W) and longer H-plasma duration (12 hour), the average diameter of the platelets is even as big as  $3.5 \mu\text{m}$  (SEM images not shown). Note that the platelets created with PECVD setup are about one order of magnitude larger than those created with remote H-plasma treatment.<sup>1,3,11</sup> However, the platelets formed with both treatments have common features, such as the formation by supersaturation of hydrogen atoms in *c*-Si, the quasi-two-dimensional structure, and the formation of Si-H bonds and H<sub>2</sub> molecules inside. Cross-section transmission electron microscopy observation confirmed the comparison of the average size of the platelets created by different hydrogenation methods.<sup>18,33</sup> We attribute this phenomenon to a much higher efficiency when introducing hydrogen into *c*-Si with PECVD rather than with remote H-plasma treatment.

Figure 2 shows the Raman spectra measured on the original surfaces (i.e., without beveling) of S1, S2, S3, and S4. It is well known that the broad peak extending from 2050 to 2150  $\text{cm}^{-1}$  reflects the stretch modes of Si-H bonds, and another one extending from 4100 to 4200  $\text{cm}^{-1}$  reflects the stretch modes of H<sub>2</sub> molecules which are located inside the platelets. Multiple subpeaks appear in the Raman spectra due to the existence of various Si-H bond or H<sub>2</sub> molecule species. Some subpeaks are indicated with dotted lines, dashed lines, or dashed-dotted-dashed lines.

We start with a general view on these spectra. Obviously, the number of the Si-H subpeaks (i.e., Si-H species) gradually decreases with increasing H-plasma duration. For instance, six subpeaks at 2065, 2075, 2095, 2105, 2120, and

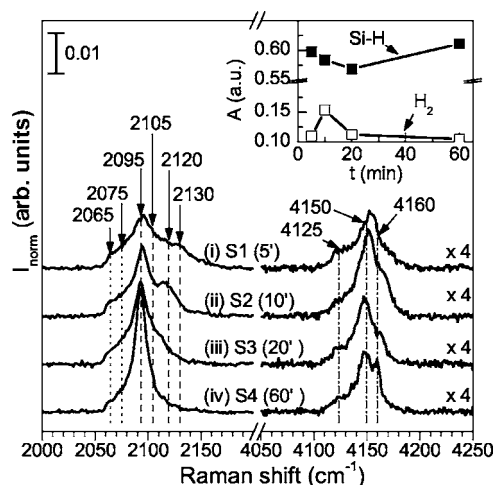


FIG. 2. Raman spectra measured on the original surfaces (i.e., without beveling) of (i) S1, (ii) S2, (iii) S3, and (iv) S4. The inset shows that the areas enveloped by the Si-H and H<sub>2</sub> peak depend on the plasma duration.

2130  $\text{cm}^{-1}$  are observed on S1 [spectrum (i)], while only four subpeaks at 2065, 2075, 2095, and 2105  $\text{cm}^{-1}$  remain on S4 [spectrum (iv)]. A detailed identification of the Si-H subpeaks will be presented somewhat below. Generally speaking, a subpeak with higher frequency indicates that it originates from SiH<sub>*n*</sub> species with higher index *n*. Additionally, it has been reported that the stretch frequency of Si-H bonds located on the surface defects (such as steps and kinks) will shift to higher values due to the steric interaction.<sup>24,26</sup> Therefore, the gradual disappearance of those subpeaks at higher frequencies with increasing plasma duration indicates that the surfaces, where the Si-H bonds are located, become flatter and contain fewer defects.

Together with the Si-H bonds, H<sub>2</sub> molecules are also observed in all samples with RS. Their subpeaks are located at about 4125, 4150, and 4160  $\text{cm}^{-1}$ . We have ascribed the two H<sub>2</sub> subpeaks at 4150 and 4160  $\text{cm}^{-1}$  to the ortho-H<sub>2</sub> molecules (with parallel nuclear spins) and to the para-H<sub>2</sub> molecules (with antiparallel nuclear spins), respectively.<sup>18,33</sup> Interestingly, most investigations carried out on the remote plasma hydrogenated *c*-Si samples only show a broad single peak instead of a clear ortho-para splitting (see, for instance, Refs. 13 and 34). This can be well explained by the effect of the platelet size, i.e., the open space where the H<sub>2</sub> molecules are trapped. Evidently, when the size is smaller, the influence of the surrounding Si atoms or Si-H bonds on the H<sub>2</sub> vibration is stronger, resulting in a larger broadness of the H<sub>2</sub> vibration spectra and therefore, an enhanced ortho-para overlap. The platelets created by remote plasma treatments are much smaller than those created by PECVD plasma treatments, so that the H<sub>2</sub> Raman subpeaks in the former case cannot be clearly distinguished. This assumption is also confirmed by the present results. For S1 (i.e., platelets with diameters in the order of  $\sim 10 \text{ nm}$ ), only a single H<sub>2</sub> peak is observed. For S2 (diameters of platelets around 150 nm), a shoulder at 4160  $\text{cm}^{-1}$  appears. While for S4 (diameters of platelets around 400 nm), the subpeaks of the ortho- and para-H<sub>2</sub> are clearly distinguished. Another subpeak at

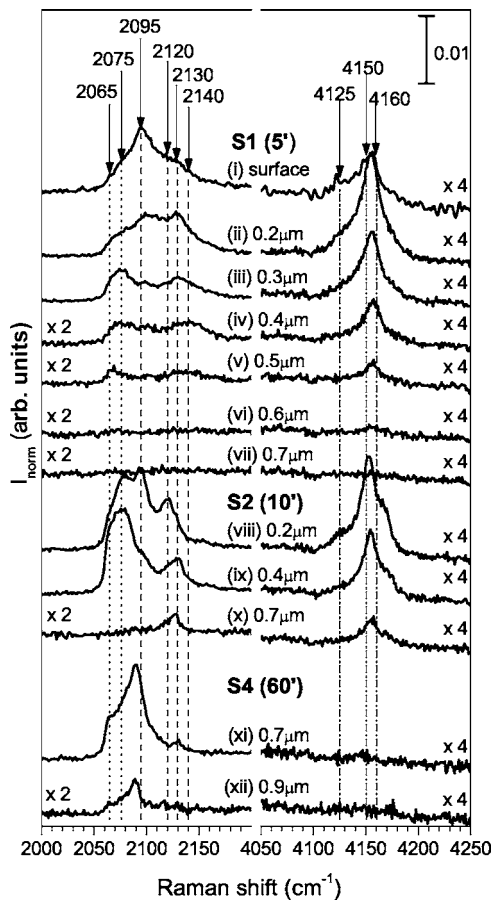


FIG. 3. Depth dependent Raman spectra measured on S1, S2, and S4. Note the different scales for the Si-H and H<sub>2</sub> spectra.

4125 cm<sup>-1</sup> has been previously discussed by Fukata *et al.*<sup>16</sup> and Leitch *et al.*<sup>13</sup> However, its origin is still not clear and remains open to further investigations.

The area enveloped by each subpeak is a measure of the concentration of the corresponding Si-H bond or H<sub>2</sub> species. Consequently the total area enveloped by the whole peak represents the overall concentration of all species of Si-H bonds or H<sub>2</sub> molecules. Shown in the inset of Fig. 2 are both concentrations of all Si-H bonds and all H<sub>2</sub> molecules depending on the H-plasma duration. We find that they do not evidently change with the H-plasma duration. However, their subpeaks are varied with the H-plasma duration, as discussed above, implying that the evolutions of the different Si-H bond or H<sub>2</sub> molecule species with H-plasma duration are different.

The concentrations of the Si-H bonds and H<sub>2</sub> molecules measured at the sample surface with RS do not evidently increase with the plasma duration, probably due to the hydrogen in-diffusion during the H-plasma treatment. Therefore, depth-resolved RS is employed. Figure 3 shows some depth dependent Raman spectra measured on S1, S2, and S4. It is found that the depth distributions of different Si-H species are different. The subpeak at 2095 cm<sup>-1</sup> only exists at depth down to  $\sim 0.2 \mu\text{m}$ , consistent with the assignment that it stems from the Si-H bonds located at a thin surface layer which is disturbed by the H-plasma.<sup>8,18</sup> The other individual

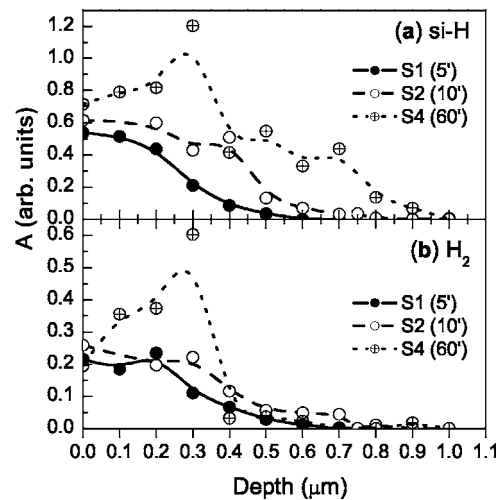


FIG. 4. Depth profile of the intensities of the (a) Si-H bonds and (b) H<sub>2</sub> molecules measured on S1, S2, and S4.

subpeaks will be discussed somewhat below in detail.

Figures 4(a) and 4(b) show the depth profiles of the concentrations of all the Si-H bonds and all H<sub>2</sub> molecules, respectively, measured on S1, S2, and S4. It is obvious that the distribution of the Si-H bonds extends to somewhat deeper wafer regions when the H-plasma duration is longer, i.e., from  $\sim 0.6 \mu\text{m}$  to  $\sim 1.0 \mu\text{m}$ , confirming the hydrogen in-diffusion during the H-plasma process. However, the depth is not proportional to the H-plasma treatment duration. Furthermore, Fig. 4(b) shows that the H<sub>2</sub> molecules are observed down to a depth of  $\sim 0.5 \mu\text{m}$  in all samples, but the concentration of the H<sub>2</sub> molecules in S4 is evidently higher than the one in S1 and S2 in the local region between 0.1 to 0.3  $\mu\text{m}$  depth. This result indicates that once the platelets are formed in the subsurface region, they act as trapping centers for the hydrogen atoms, so that the growth of platelets is suppressed in deeper sample regions due to the lack of hydrogen. Recently, we have also found that the trapping of hydrogen by platelets results in a decrease of the apparent hydrogen diffusivity.<sup>35</sup>

#### IV. DISCUSSION

As mentioned in the Introduction, H<sub>2</sub> molecules are formed in the open space of the platelets. The dangling bonds of the inner surfaces of the platelets are passivated by hydrogen atoms, since the formation of Si-H bonds is energetically more favorable than the formation of H<sub>2</sub> molecules. We find that the Si-H bond species on the inner surfaces of the platelets depends on the growth stage of the platelets (see below). In this section, we will determine those subpeaks which stem from the Si-H bonds located on the inner surfaces of the platelets, via a combined analysis of the Si-H and H<sub>2</sub> Raman spectra. After that, we can deduce the species of the Si-H bonds and even the morphology of the inner surfaces, since both of them will result in specific Si-H vibration frequency. A detailed discussion will follow.

##### Subpeak at 2065 and 2075 cm<sup>-1</sup>

As shown in Fig. 1, the subpeaks at 2065 and 2075 cm<sup>-1</sup> are observed in the Raman spectra measured on the surfaces

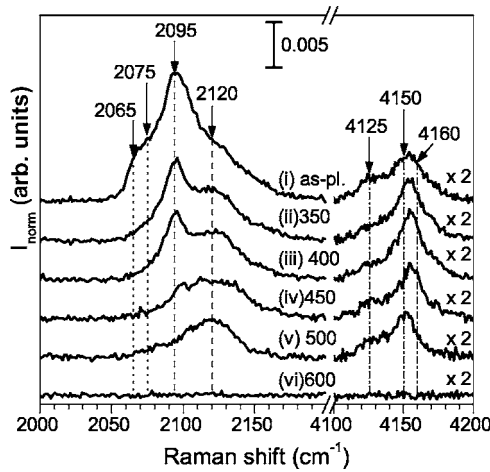


FIG. 5. Raman spectra measured on the as-plasma treated and annealed S1. The annealing was done for 20 min at various temperatures between 350 °C to 600 °C.

of all hydrogenated samples. It is found that the intensities of these two subpeaks are almost independent on the duration of the H-plasma treatments. Furthermore, depth-resolved RS shows that the two subpeaks exist not only on the surface, but also in quite deep wafer regions. For example, both subpeaks appear at the depth of 0.7 and 0.9  $\mu\text{m}$  in S4, as indicated in Fig. 3(xi) and (xii), respectively. It is found that both subpeaks are not associated with  $\text{H}_2$  molecules. For instance, Fig. 3(xii) significantly exhibits the two subpeaks, while no  $\text{H}_2$  peak can be observed. Furthermore, Figs. 3(iii) and 3(v) clearly show that both of them are discernable individual subpeaks, rather than a tail of subpeaks with higher frequencies. The evolutions of both subpeaks under thermal annealing are also investigated. The results are shown in Fig. 5. It is found that the subpeaks at 2065 and 2075  $\text{cm}^{-1}$  are less stable than other Si-H subpeaks. They disappear upon annealing at 350 °C for 20 min.

We first discuss the origin of the subpeak at 2065  $\text{cm}^{-1}$ . The vibration frequencies of the multivacancy-H complexes fall into the spectrum regime which is close to this subpeak. Johannesen *et al.* observed two IR absorption peaks at 2068.1 and 2073.2  $\text{cm}^{-1}$  on the hydrogen implanted *c*-Si sample at a measurement temperature of 10 K. They assigned to the peaks to the  $\text{V}_2\text{H}$  (2068.1  $\text{cm}^{-1}$ ) and  $\text{V}_3\text{H}$  or  $\text{V}_4\text{H}$  (2073.2  $\text{cm}^{-1}$ ).<sup>36</sup> Recently, Shinohara *et al.* observed an IR peak at 2060  $\text{cm}^{-1}$  on a remote H-plasma treated *c*-Si sample, and they attributed it to the hydrogen terminated vacancies.<sup>37</sup> In a previous investigation we assigned a Raman subpeak at  $\sim 2070$   $\text{cm}^{-1}$ , which was measured on the PECVD hydrogenated *c*-Si samples, to the monovacancy-hydrogen (VH) complex, since it was found that this subpeak had a similar thermal stability as that of VH.<sup>8</sup> However, the above assignment of the subpeak at  $\sim 2065$   $\text{cm}^{-1}$  observed on the plasma hydrogenated *c*-Si samples to the V-H complexes is quite doubtful, since vacancies cannot be significantly created either with remote H-plasma or PECVD treatment. We find that the self-bias voltage, which can be considered as the maximum energy that the ions could gain, is less than 10 V during the H-plasma treatment with our

employed PECVD setup. This is much lower than the threshold energy for the creation of a Si Frenkel pair by both  $\text{H}^+$  ( $\sim 110$  eV) and  $\text{H}_2^+$  ( $\sim 60$  eV) ions.<sup>38</sup> Furthermore, the existence of this subpeak in a quite deep wafer region [0.5  $\mu\text{m}$  in Fig. 3(v), 0.9  $\mu\text{m}$  in Fig. 3(xii)] will *definitely* rule out its assignment to any V-H complex (a projected range of 0.9  $\mu\text{m}$  requires a hydrogen energy of approximately 90 keV).

Weldon *et al.*<sup>30</sup> have reported that after bonding of two atomically flat, ideally hydrogen terminated Si(111) wafers prepared by wet-etching, an IR absorption peak at 2065  $\text{cm}^{-1}$  is observed. Thus they attributed this peak to the disturbed mode of the monohydride (SiH) on the Si(111) surface. *Ab initio* calculations showed that the two bonded Si(111) surfaces could come sufficiently close to each other due to the influence of the van der Waals attraction, and that the interaction between opposite hydrogen atoms would reduce the vibration frequency of the undisturbed mode at 2083.5  $\text{cm}^{-1}$  to the measured one at 2063  $\text{cm}^{-1}$ .<sup>30</sup> This result becomes an intriguing solution for the subpeak at 2065  $\text{cm}^{-1}$  observed in our plasma hydrogenated *c*-Si samples, if we take into account the formation of the platelets.

There have been a number of theoretical attempts to predict the microscopic structure of platelets.<sup>39–42</sup> Among those, Deák *et al.*<sup>39</sup> suggested that pairs of hydrogen atoms saturating broken bonds between adjacent planes are the most stable arrangement; this structure is known as the  $[\text{2Si-H}]_n$  structure. This scenario will fit our results excellently, if the (111) platelets formed in the plasma hydrogenated *c*-Si have the structure as proposed by Deák *et al.* The inner surfaces of the platelets are passivated by the SiH, and separated by several Å. As was theoretically and experimentally investigated by Weldon *et al.*,<sup>30</sup> the frequency of the SiH is shifted to the lower value of  $\sim 2065$   $\text{cm}^{-1}$  due to the interaction of opposite hydrogen atoms. This frequency is just the one which was observed by Shinohara *et al.*<sup>37</sup> and by us with IR and RS analysis, respectively, on the plasma hydrogenated *c*-Si samples. Furthermore, according to the  $[\text{2Si-H}]_n$  structure, no  $\text{H}_2$  molecules are trapped inside, in agreement with our observation that the subpeak at 2065  $\text{cm}^{-1}$  is not associated with  $\text{H}_2$  molecules.

Kim *et al.* calculated that a pure  $[\text{2Si-H}]_n$  structure is a metastable configuration.<sup>41</sup> With further plasma treatment or thermal annealing hydrogen could be trapped inside, and  $\text{H}_2$  molecules were formed, i.e., the pure  $[\text{2Si-H}]_n$  structure would be transformed to  $[\text{2Si-H}]_n + \text{H}_2$  structure or even to larger defects.<sup>41</sup> This is consistent with our observations that the subpeaks at 2065 and 2075  $\text{cm}^{-1}$  are less stable than other subpeaks (see Fig. 5). The metastability of the pure  $[\text{2Si-H}]_n$  structure implies that its concentration has an upper limit, in agreement with our experimental result that the intensity of the subpeak at 2065  $\text{cm}^{-1}$  does not depend on the H-plasma duration (see Fig. 1).

A slight increase of the distance between the inner surfaces of the  $[\text{2Si-H}]_n$  structure will result in a weakening of the interaction between opposite hydrogen atoms, i.e., the vibration frequencies of the SiH will increase and finally return to the value of its relaxed state at 2083  $\text{cm}^{-1}$  when the distance is larger than  $\sim 8$  Å.<sup>30</sup> Hence, we suggest that the

subpeak at  $2075\text{ cm}^{-1}$  stems from those  $[2\text{Si-H}]_n$  structures with medium distances between two inner surfaces. Indeed, in Figs. 2 and 3 this subpeak is more like a wide band, indicating a variation of the distances between the inner surfaces.

It is hard to believe that the subpeak at  $2065\text{ cm}^{-1}$  stems from the  $\text{H}_2^*$  defects (the  $\text{H}_2^*$  defect is defined as a pair of  $\text{H}_{AB}$ - $\text{H}_{BC}$ , where  $\text{H}_{AB}$  and  $\text{H}_{BC}$  represent hydrogen atom located at the antibond center and bond center site, respectively). This is because this defect exhibits two IR peaks at  $1832$  and  $2053\text{ cm}^{-1}$  (at room temperature), which originate from  $\text{H}_{AB}$ -Si and  $\text{H}_{BC}$ -Si, respectively.<sup>43</sup> However we do not find any Raman peak near  $1832\text{ cm}^{-1}$  at all (IR and Raman have identical active modes for the  $\text{H}_2^*$  defect, which belongs to  $C_{3v}$  point group).<sup>44-46</sup>

#### Subpeak at 2130 and 2140 $\text{cm}^{-1}$

As shown in Fig. 2(i), the subpeak at  $2130\text{ cm}^{-1}$  appears as a pronounced shoulder in the Raman spectrum measured on the surface of S1. This subpeak is not observed on the surfaces of other three samples treated with longer plasma durations. In a certain depth region of S1 [say, at about  $0.2$  and  $0.3\ \mu\text{m}$ , as shown in Figs. 3(ii) and 3(iii) respectively], this subpeak becomes dominant. This subpeak also evidently exists in the regions between  $0.4$ – $0.7\ \mu\text{m}$  of S2 [see Figs. 3(ix) and 3(x)]. Furthermore, Fig. 3(x) shows only one subpeak at  $2130\text{ cm}^{-1}$ . Simultaneously the  $\text{H}_2$  peak is also observed, indicating that the subpeak at  $2130\text{ cm}^{-1}$  stems from the inner surfaces of the platelets, which contain  $\text{H}_2$  molecules. As shown in Fig. 3(iv), we observe the  $\text{H}_2$  peak, as well as three Si-H subpeaks at  $2065$ ,  $2075$ , and  $2140\text{ cm}^{-1}$ . In the above discussion we have pointed out that the former two subpeaks are not associated with  $\text{H}_2$  molecules, so we can conclude that the subpeak at  $2140\text{ cm}^{-1}$  stems from the inner surfaces of platelets, which contain  $\text{H}_2$  molecules. Since the two subpeaks at  $2130$  and  $2140\text{ cm}^{-1}$  are observed either on the surfaces of the samples treated with a short time H-plasma exposure, or on the samples with longer H-plasma exposure but in deeper sample regions, we suggest that they stem from those Si-H bonds located on the inner surfaces of the platelets formed in an early stage.

Now we discuss the Si-H species related to the two subpeaks. Chabel *et al.*<sup>24</sup> observed an IR peak at  $2139\text{ cm}^{-1}$  on the HF etched both flat and stepped Si(111) surfaces, and assigned this IR peak to the asymmetric stretch mode of the trihydride ( $\text{SiH}_3$ ). Based on the *ab initio* cluster calculation, they found that the symmetric stretch mode of  $\text{SiH}_3$  would be about  $10\text{ cm}^{-1}$  lower than asymmetric mode, i.e., at about  $\sim 2130\text{ cm}^{-1}$ . Jansson *et al.*<sup>47</sup> found an IR peak at  $2143\text{ cm}^{-1}$  on the Si(111) surface after high UHV (ultrahigh vacuum) hydrogen exposure, and also assigned it to  $\text{SiH}_3$  formed on the sample surface. Stein *et al.*<sup>48</sup> observed an IR peak at  $2142\text{ cm}^{-1}$  on the H-plasma exposed *c*-Si samples and followed the above assignment.

However, Jakob *et al.*<sup>26</sup> proposed alternative assignments. They considered the steric interaction between hydrogen atoms in a stepped structure, which was formed by a  $9^\circ$  miscut off the (111) plane in the  $\langle -1-12 \rangle$  direction. The authors cal-

culated the steric interaction between the hydrogen atoms of the lower Si-H bond of the vertical  $\text{SiH}_2$ , and of the SiH located directly below the step on the lower terrace. It was found that due to this steric interaction the stretch frequencies of both involved SiH and  $\text{SiH}_2$  were higher than typical SiH and  $\text{SiH}_2$  frequencies. Explicitly, they assigned the measured IR peak at  $2134.7\text{ cm}^{-1}$  to the stretch mode of the lower Si-H bond of the vertical  $\text{SiH}_2$ . Watanabe<sup>29</sup> followed this explanation. He attributed an IR peak at  $2139.9\text{ cm}^{-1}$ , which was measured on the HF etched Si(110) surface, to the strained vertical  $\text{SiH}_2$ .

The above discussion shows that some controversy still exists on the definite assignment of the subpeaks around  $2130$  and  $2140\text{ cm}^{-1}$ . Following the above studies, we assign the Raman subpeaks at  $2130$  and  $2140\text{ cm}^{-1}$  either to the vertical  $\text{SiH}_2$  on the steps or to the  $\text{SiH}_3$ . They are located on the inner surfaces of the platelets formed in an early stage, which contain  $\text{H}_2$  molecules. Obviously, the presence of the vertical  $\text{SiH}_2$  or  $\text{SiH}_3$  species indicates that the inner surfaces of those platelets are quite rough. The fairly large width of the subpeak at  $2130$  and  $2140\text{ cm}^{-1}$  is a further hint for this conclusion.

#### Subpeak at 2105 and 2120 $\text{cm}^{-1}$

In a previous study,<sup>9</sup> we assigned a Raman subpeak at  $2105\text{ cm}^{-1}$  to the dihydride ( $\text{SiH}_2$ ) at the inner surfaces of the platelets formed in plasma hydrogenated *c*-Si samples. It was found that this subpeak became dominant in the hydrogenated samples upon annealing at  $450^\circ\text{C}$  for 90 min, representing the most stable hydride species formed at the inner surfaces of the platelets. Therefore, the appearance of this subpeak means that a quite large and stable platelet has formed at the final stage. In this study the subpeak at  $2105\text{ cm}^{-1}$  exists only as a weak shoulder both on the as-plasma treated or annealed samples (see Figs. 2 and 5), possibly because the plasma power on these samples ( $10\text{ W}$ ) is much lower than the one on the previous samples ( $50\text{ W}$ ) so that the formed platelets are also smaller.

As shown in Fig. 2, the subpeak at  $\sim 2120\text{ cm}^{-1}$  is weakly present as a shoulder in spectrum (i) (i.e., S1), and remarkably on spectrum (ii) (i.e., S2). However, this subpeak does not appear on the surfaces of the samples hydrogenated with longer durations. In case of depth-dependent Raman spectra (Fig. 3), this subpeak becomes a predominant subpeak on spectrum (viii), which is measured at a depth of  $0.2\ \mu\text{m}$  of S2. Furthermore, as shown in Fig. 5, it becomes the dominant subpeak upon annealing at elevated temperatures. The  $\text{H}_2$  subpeak is also observed in Figs. 5(i)–5(v). As a consequence, we conclude that the Si-H species related to the subpeak at  $2120\text{ cm}^{-1}$  is located on the inner surfaces of the platelets formed at an intermediate stage. The platelets contain  $\text{H}_2$  molecules. Its assignment is somewhat less controversial than other subpeaks. Chabel *et al.* observed an IR peak at  $2117\text{ cm}^{-1}$  on both wet HF etched<sup>24</sup> and water exposed<sup>19</sup> *c*-Si samples, and they assigned it to the  $\text{SiH}_2$ . On the UHV hydrogen exposed Si(111) surface, Jansson *et al.* observed an IR peak at  $2119\text{ cm}^{-1}$ , and they attributed it to the  $\text{SiH}_2$  stretch mode.<sup>47</sup> Hence, we assign the subpeak at

2120  $\text{cm}^{-1}$  to the  $\text{SiH}_2$ , which is located on the inner surfaces of platelets formed at an intermediate stage. In addition, Fig. 5 reveals that under annealing the subpeak at 2095  $\text{cm}^{-1}$  disappears at lower temperatures as compared to the subpeak at 2120  $\text{cm}^{-1}$ , in agreement with the conclusion that the Si-H bonds at the H-plasma disturbed thin surface layer are less stable than those at the inner surfaces of the platelets.<sup>9</sup>

## V. CONCLUSION

The hydride formation on the inner surfaces of the platelets in PECVD plasma hydrogenated *c*-Si materials is investigated with RS. Several Si-H Raman subpeaks at 2065, 2075, 2105, 2120, 2130, and 2140  $\text{cm}^{-1}$  are found to be related to the different growth stages of the platelets. Based on the results and discussion, we suggest that the  $[\text{2Si-H}]_n$  structure is the initial nucleus for the  $\{111\}$  platelet formation. The stretch frequency of SiH located on the inner sur-

faces of this structure is significantly lower than the one of normal SiH, because of the interaction between the opposite hydrogen atoms. No  $\text{H}_2$  molecules are formed inside this structure. This structure is a metastable configuration. With longer H-plasma treatments or thermal annealing they grow to platelets with  $\text{H}_2$  molecules formed inside. At this stage the inner surfaces of the platelets are quite rough, characterized by the vertical  $\text{SiH}_2$  or  $\text{SiH}_3$  formation. When more H atoms are trapped inside either by further H-plasma treatments or thermal annealing, the inner surfaces of the platelets become flatter and less defective, represented by the normal  $\text{SiH}_2$  formation.

## ACKNOWLEDGMENTS

The authors are grateful to Katrina Meusinger and Boguslaw Wdowiak for technical support. The financial support of the German Academic Exchange Service (DAAD) is gratefully acknowledged by the authors Y.M., Y.L.H., and W.R.F.

- 
- <sup>1</sup>N. M. Johnson, F. A. Ponce, R. A. Street, and R. J. Nemanich, *Phys. Rev. B* **35**, 4166 (1987).  
<sup>2</sup>N. M. Johnson, C. Herring, C. Doland, J. Walker, G. Anderson, and F. Ponce, *Mater. Sci. Forum* **83–87**, 33 (1992).  
<sup>3</sup>K. H. Hwang, E. Yoon, K. W. Whang, and J. Y. Lee, *Appl. Phys. Lett.* **67**, 3590 (1995).  
<sup>4</sup>A. W. R. Leitch, V. Alex, and J. Weber, *Phys. Rev. Lett.* **81**, 421 (1998).  
<sup>5</sup>A. W. R. Leitch, J. Weber, and V. Alex, *Mater. Sci. Eng., B* **B58**, 6 (1999).  
<sup>6</sup>S. Muto, S. Takeda, and M. Hirata, *Philos. Mag. A* **72**, 1057 (1995).  
<sup>7</sup>J. Grisolia, G. B. Assayag, and A. Claverie, *Appl. Phys. Lett.* **76**, 852 (2000).  
<sup>8</sup>Y. Ma, Y. L. Huang, R. Job, and W. R. Fahrner, *Electrochem. Soc. Proc.* **2004-05**, 385 (2004).  
<sup>9</sup>Y. Ma, Y. L. Huang, R. Job, and W. R. Fahrner, *Phys. Rev. B* **71**, 045206 (2005).  
<sup>10</sup>N. H. Nickel, G. B. Anderson, and J. Walker, *Solid State Commun.* **99**, 427 (1996).  
<sup>11</sup>N. H. Nickel, G. B. Anderson, N. M. Johnson, and J. Walker, *Physica B* **273–274**, 212 (1999).  
<sup>12</sup>M. Kitajima, K. Ishioka, S. Tateishi, K. Nakanoya, N. Fukata, K. Murakami, S. Fujimura, S. Hishita, M. Komatsu, and H. Haneda, *Mater. Sci. Eng., B* **B58**, 13 (1999).  
<sup>13</sup>A. W. R. Leitch, V. Alex, and J. Weber, *Solid State Commun.* **105**, 215 (1998).  
<sup>14</sup>M. Kitajima, K. Ishioka, K. Murakami, K. Nakanoya, and T. Mori, *Physica B* **273–274**, 192 (1999).  
<sup>15</sup>N. H. Nickel, G. B. Anderson, N. M. Johnson, and J. Walker, *Phys. Rev. B* **62**, 8012 (2000).  
<sup>16</sup>N. Fukata, S. Sasaki, K. Murakami, K. Ishioka, K. G. Nakamura, M. Kitajima, S. Fujimura, J. Kikuchi, and H. Haneda, *Phys. Rev. B* **56**, 6642 (1997).  
<sup>17</sup>M. Kitajima, K. Ishioka, K. Nakanoya, S. Tateishi, T. Mori, N. Fukata, K. Murakami, and S. Hishita, *Jpn. J. Appl. Phys., Part 2* **38**, L691 (1999).  
<sup>18</sup>Y. Ma, R. Job, Y. L. Huang, W. R. Fahrner, M. F. Beaufort, and J. F. Barbot, *J. Electrochem. Soc.* **151**, G627 (2004).  
<sup>19</sup>Y. J. Chabal, *Phys. Rev. B* **29**, 3677 (1984).  
<sup>20</sup>Y. J. Chabal and K. Raghavachari, *Phys. Rev. Lett.* **53**, 282 (1984).  
<sup>21</sup>Y. J. Chabal and K. Raghavachari, *Phys. Rev. Lett.* **54**, 1055 (1985).  
<sup>22</sup>P. Gupta, V. L. Colvin, and S. M. George, *Phys. Rev. B* **37**, 8234 (1988).  
<sup>23</sup>V. A. Burrows, Y. J. Chabal, G. S. Higashi, K. Raghavachari, and S. B. Christman, *Appl. Phys. Lett.* **53**, 998 (1988).  
<sup>24</sup>Y. J. Chabal, G. S. Higashi, and K. Raghavachari, *J. Vac. Sci. Technol. A* **7**, 2104 (1989).  
<sup>25</sup>G. S. Higashi, Y. J. Chabal, G. W. Trucks, and K. Raghavachari, *Appl. Phys. Lett.* **56**, 656 (1990).  
<sup>26</sup>P. Jakob and Y. J. Chabal, *J. Chem. Phys.* **95**, 2897 (1991).  
<sup>27</sup>M. A. Hines, Y. J. Chabal, T. D. Harris, and A. L. Harris, *J. Chem. Phys.* **101**, 8055 (1994).  
<sup>28</sup>H. Bender, S. Verhaverbeke, and M. M. Heyns, *J. Electrochem. Soc.* **141**, 3128 (1994).  
<sup>29</sup>S. Watanabe, *Surf. Sci.* **351**, 149 (1996).  
<sup>30</sup>M. K. Weldon, Y. J. Chabal, D. R. Hamann, S. B. Christman, E. Chaban, and L. C. Feldman, *J. Vac. Sci. Technol. B* **14**, 3095 (1996).  
<sup>31</sup>D. B. Fenner, D. K. Biegelsen, and R. D. Bringans, *J. Appl. Phys.* **66**, 419 (1989).  
<sup>32</sup>T. Miura, M. Niwano, D. Shoji, and N. Miyamoto, *J. Appl. Phys.* **79**, 4373 (1996).  
<sup>33</sup>R. Job, A. G. Ulyashin, W. R. Fahrner, M. F. Beaufort, and J. F. Barbot, *Eur. Phys. J.: Appl. Phys.* **23**, 25 (2003).  
<sup>34</sup>K. Murakami, N. Fukata, S. Sasaki, K. Ishioka, M. Kitajima, S. Fujimura, J. Kikuchi, and H. Haneda, *Phys. Rev. Lett.* **77**, 3161 (1996).  
<sup>35</sup>Y. L. Huang, Y. Ma, R. Job, and W. R. Fahrner, *Appl. Phys. Lett.* **86**, 131911 (2005).

- <sup>36</sup>P. Johannesen, R. Jakobsen, P. Stallinga, B. Bech Nielsen, and J. R. Byberg, *Phys. Rev. B* **66**, 235201 (2002).
- <sup>37</sup>M. Shinohara, T. Kuwano, Y. Akama, Y. Kimura, and M. Niwano, *J. Vac. Sci. Technol. A* **21**, 25 (2003).
- <sup>38</sup>D. Bräunig and W. R. Fahrner, in *Instabilities in Silicon Devices Volume 2, Silicon Passivation and Related Instabilities*, edited by G. Barbottin (Elsevier Science, Amsterdam, The Netherlands, 1989), Vol. 1, p. 12.
- <sup>39</sup>P. Deák, C. R. Ortiz, L. C. Snyder, and J. W. Corbett, *Physica B* **170**, 223 (1991).
- <sup>40</sup>S. B. Zhang and W. B. Jackson, *Phys. Rev. B* **43**, R12142 (1991).
- <sup>41</sup>Y. S. Kim and K. J. Chang, *Phys. Rev. Lett.* **86**, 1773 (2001).
- <sup>42</sup>F. A. Reboredo, M. Ferconi, and S. T. Pantelides, *Phys. Rev. Lett.* **82**, 4870 (1999).
- <sup>43</sup>M. Suezawa, N. Fukata, T. Takahashi, M. Saito, and H. Yamada-Kaneta, *Phys. Rev. B* **64**, 085205 (2001).
- <sup>44</sup>J. D. Holbeck, B. Bech Nielsen, R. Jones, P. Sitch, and S. Öberg, *Phys. Rev. Lett.* **71**, 875 (1993).
- <sup>45</sup>B. Schrader, in *Infrared and Raman Spectroscopy*, edited by B. Schrader (VCH Verlagsgesellschaft mbH, Weinheim, Germany, 1995), p. 43.
- <sup>46</sup>*Introduction to Infrared and Raman Spectroscopy*, 3rd ed., edited by N. B. Colthup, L. H. Daly, and S. E. Wiberley (Academic, San Diego, 1990), p. 150.
- <sup>47</sup>U. Jansson and K. J. Uram, *J. Chem. Phys.* **91**, 7978 (1989).
- <sup>48</sup>H. J. Stein, S. M. Myers, and D. M. Follstaedt, *J. Appl. Phys.* **73**, 2755 (1993).